Toward Autonomous Free-Climbing Robots

Tim Bretl[1], Jean-Claude Latombe[2], and Stephen Rock[1]

[1] Aerospace Robotics Lab, Department of Aeronautics and Astronautics
[2] Robotics Laboratory, Computer Science Department
Stanford University, Stanford CA 94305, USA
{tbretl,rock}@sun-valley.stanford.edu, latombe@cs.stanford.edu

Abstract. The goal of this research is to enable a multi-limbed robot to climb vertical rock using techniques similar to those developed by human climbers. The robot consists of a small number of articulated limbs. Only the limb end-points can make contact with the environment—a vertical surface with small, arbitrarily distributed features called holds. A path through this environment is a sequence of *one-step climbing moves* in which the robot brings a limb end-point to a new hold. The robot maintains balance during each move by pushing and/or pulling at other holds, exploiting contact and friction at these holds while adjusting internal degrees of freedom to avoid sliding. The paper first considers a planar three-limbed robot, then a 3-D four-limbed robot modeled after a real hardware system. It proposes an efficient test of the quasi-static equilibrium of these robots and describes a fast planner based on this test to compute one-step climbing moves. This planner is demonstrated in simulation for both robots.

1 Introduction

Our goal is to enable a multi-limbed robot to climb vertical rock using skills and techniques similar to those developed by human climbers (see Fig. 1). We refer here to "free-climbing" techniques, where the climber only uses natural features and friction of the terrain for upward progress. These techniques are in contrast to "aid climbing," where the climber relies on additional gear for progress [18]. The robots we consider consist of a small number of articulated limbs attached to a pelvis (see Fig. 2). Only the limb end-points make contact with the environment—a vertical surface with small, arbitrarily distributed features (e.g., protrusions, holes) called *holds*. A *one-step climbing move* for the robot consists of bringing a limb endpoint to a new hold while maintaining balance by pushing or pulling at other holds [9]. The robot exploits friction at these holds while adjusting internal degrees of freedom (DOF's) to avoid sliding.

Humans have not been created, nor have they evolved to climb vertical rock. Nevertheless, some climb steep rock surfaces, with small and sparse holds. In fact, natural vertical terrain may often be climbed without significant strength by using balancing techniques known as stem, back-step, lie-back, etc., which share one idea—opposition—i.e., exert two opposing forces against each other [18]. Similarly, we do not intend to design a new robot for rock-climbing activities. Instead, our goal is to develop generic control, planning, and sensing capabilities to enable a wide class of multi-limbed robots to climb vertical terrain.

The availability of non-specific autonomous rock-climbing robots could benefit several application areas. These include search-and-rescue in mountainous terrain or broken urban environments, exploration of sub-surface environments such as caves, and planetary exploration, particularly on Mars where sites with potentially high science value have been identified on cliff faces. This research may also yield the discovery of new modes of mobility for limbed robots. Indeed, human climbers often report on discovering "new degrees of freedom" providing increased balance and range of movement in everyday activity.

This paper focuses on the problem of computing the one-step climbing moves of multi-limbed robots. Motion is assumed quasi-static, as is usually the case in human climbing. Section 3 studies this problem for a planar three-limbed robot. Section 4 considers a more complex 3-D four-limbed robot. Both sections give simulation results obtained with the implemented software. Our current goal is to implement the results of Section 4 on a real robot, "LEMUR II", created by the Jet Propulsion Laboratory [27, 28].

2 Previous Related Work

2.1 Climbing robots

Various robots capable of climbing vertical *artificial* surfaces have been proposed:

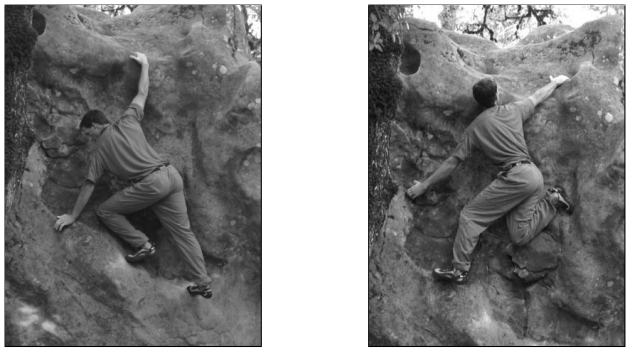

(a) High-Step (b) Back-Step

Fig. 1. Typical configurations of a human climber.

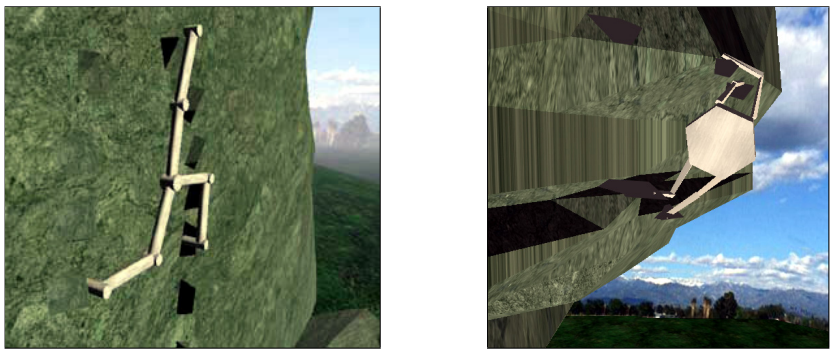

(a) (b)

Fig. 2. Simulation of three-limbed and four-limbed robots.

1. Robots that "stick" to a featureless, flat or smoothly curved surface by using specific end-effectors—e.g., suction cups and pads, or magnets—exploiting a uniform property of the surface [19, 22]. Applications include cleaning, painting, and inspection of building facades and ship hulls.
2. Robots whose end-effectors exploit features of the environment—e.g., holes (in which they insert peg-shaped end-effectors) [5, 52], handrails or bars [1], and poles [47]. Applications include construction, inspection, and repair of truss structures, like space stations, electricity pylons, and bridges.
3. Robots designed to climb within pipes and ducts [34, 39, 48]. These are multi-limbed robots that, like in our work, exploit friction by pushing at multiple contact points along opposite directions. But the regularity of the environment allows them to use pre-computed, gaited motions.

These robots exploit surface properties that are not available in natural terrain. To our knowledge, there has been little research on robots climbing vertical natural terrain. An exception is the Gecko robot of iRobot which is inspired from the adhesion mechanism in gecko toes [2, 25].

2.2 Track and legged robots

Wheeled and track rovers have been used to ascend natural slopes of up to 50 degrees, and to climb over small obstacles in rough terrain. They use a variety of techniques, such as tracks that conform to the shape of the terrain [56], active or rocker-bogie suspension [13, 24, 50], and rappelling [43]. None of these techniques scale up to vertical terrain.

Similar results have been obtained using legged robots [3, 23, 42, 55] and snake-like robots [41, 54]. The legged robots, in particular, are like those considered in our work. They must move one (or several) limbs at a time, while using contacts of the other limbs with the terrain to remain stable. However, on flat or sloped terrain, many legged robots use predefined gaits that adapt reactively to sensory inputs such as contact detection [29, 32, 37, 42, 51, 53]. On steep, irregular terrain, predefined gaits are not possible. Instead, the robot must choose carefully where to place its feet.

Fewer works consider the problem of foot-placement. Algorithms in [7, 12, 21, 30, 31] are based on assumptions that are not valid for climbing vertical terrain. In particular, in [7, 21] legs are assumed

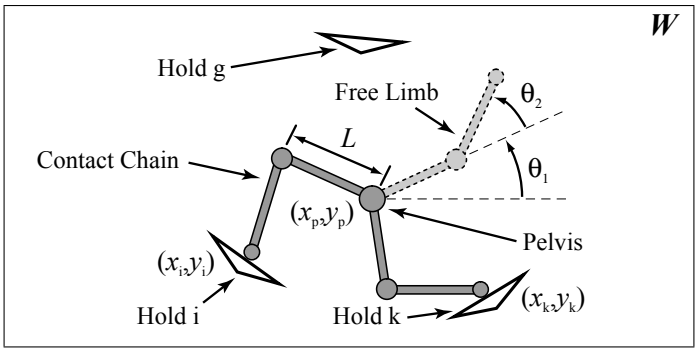

Fig. 3. Three-limbed climbing robot.

massless and friction is not modeled. In [30, 31] a randomized planner computes dynamically-stable motions of a humanoid biped robot among obstacles, but considers horizontal foot-placements only. Motion strategies for a planar quadruped robot are given in [45], but are restricted to horizontal tunnels, and require form-closure configurations during each motion step.

2.3 Grasping and multi-fingered manipulation

The relationship between multi-fingered manipulation and legged locomotion has been established before (e.g., in [45]). While a robot hand grasps an object, a legged robot "grasps" its environment. A multi-step motion of a legged robot is loosely similar to re-grasping an object by successively re-positioning fingers on the object. The same relation exists with a multi-limbed climbing robot.

A key concept in grasping is force-closure. A grasp is force-closure if it can resist forces (and torques) applied to the object along (about) any direction [6]. The smallest number of fingers needed to achieve closure of an arbitrary object has been studied for various models of contacts [35, 38, 46]. Algorithms for computing force-closure grasps of given objects are described in [11, 16, 40, 44].

However, a climbing robot need not achieve force-closure, since it must only resist gravity. Moreover, when a climbing robot's limb moves to reach a new hold, the robot itself must remain in equilibrium during the motion as its center of mass changes. In contrast, when fingers are re-positioned on an object, the object is what needs to remain in equilibrium, but its center of mass does not change.

3 Planar Three-Limbed Robot

3.1 Model and problem

The robot (see Fig. 3) moves in a vertical plane W. It consists of three identical limbs meeting at a point called the *pelvis*. Each limb has two links and two actuated revolute joints, one located at the pelvis, the other between the two links. We ignore self-collision, meaning that we allow links to cross each other. We also assume all six links have equal mass and equal length L, and that joints are not limited by any internal mechanical stops. A fixed coordinate system O_{xy} is embedded in W, with gravity pointing in the negative direction of the y-axis. Any configuration of the robot can be defined by 8 parameters, the coordinates (x_p, y_p) of the pelvis and the joint angles (θ_1, θ_2) of each limb.

The plane W contains scattered *holds*. Each hold i is defined by a point (x_i, y_i) and a direction ν_i. In figures, it is depicted as an elongated isosceles triangle; but the hold itself is located at the midpoint of the long edge of the triangle and is oriented along the outgoing normal to this edge. The endpoint of each limb of the robot is called a *foot*. In Fig. 3, two feet are at holds i and k, respectively, while the third limb is moving. The holds i and k are the *supporting* holds. The two-limbed linkage between i and k is called the *contact chain* and the other limb the *free limb*. The motion takes place in a 4-D subspace C_{ik} of the robot's configuration space, since the fixed positions of two feet at the supporting holds reduce the number of DOFs of the contact chain to 2.

Friction at each hold is modeled using Coulomb's law. If a foot is located at hold i, the reaction force $\boldsymbol{f}_i$ that the hold may exert on the foot spans a cone FC_i—the *friction cone* at i—of half-angle $\varphi_i \leq \pi/2$. The apex of this cone is at (x_i, y_i) and its main axis points along ν_i. For the robot to be in quasi-static equilibrium, there must exist reaction forces at the supporting holds whose sum exactly compensates for the gravitational force on the robot. (Henceforth, for simplicity, "equilibrium" will always mean "quasi-static equilibrium.")

We consider the following problem:

One-Step-Climbing Problem. Given a start configuration q_s of the robot in C_{ik} and a hold g, compute a path of the robot connecting q_s to a configuration that places the foot of the free limb at hold g and such that the robot remains in equilibrium along the entire path.

3.2 Motion computation (basic algorithm)

Let F_{ik} denote the subset of C_{ik} where the robot is in equilibrium. We call it the *feasible space* at holds i and k. A solution path, if one exists, must lie in F_{ik}. A PRM (Probabilistic RoadMap) motion planning approach [26] can be used to compute such a path. For most PRM planners, the feasible space consists of collision-free configurations. Here, it is made of equilibrium configurations. But this does not change the general planning approach. See [31] for a prior PRM planner that handles equilibrium constraints.

The planner samples configurations at random from C_{ik} (including the start configuration q_s among them). It retains each sampled configuration where the robot is in equilibrium as a vertex of the roadmap. (An efficient equilibrium test will be described in Section 3.3.) In addition, for any two vertices that are sufficiently close, if the robot remains in equilibrium along the linear path joining them, then the planner retains the path as an edge of the roadmap. The planner builds the roadmap until either the connected component containing q_s also contains a configuration that places the foot of the free limb at g, or the roadmap reaches a pre-specified maximal size, in which case the planner returns failure.

Thus, the planner must sample configurations of the contact chain. The problem of sampling configurations of a closed-loop kinematic chain has been addressed in [10, 20, 33]. Here, it is solved in a simple fashion: C_{ik} is divided into four disjoint regions, each corresponding to a distinct combination of "knee bends" of the two limbs forming the contact chain. The knee bend of a limb is the sign of its joint angle θ_2. In each region, a configuration is uniquely specified by four parameters: the pelvis coordinates (x_p, y_p) and the free-limb joint angles (θ_1, θ_2). To sample a configuration, we pick the values of the two knee bends and the values of the four parameters x_p, y_p, θ_1, and θ_2 independently at random. The values of (x_p, y_p) are sampled in the intersection of the two discs of radius $2L$ centered at holds i and k, respectively.

In general, the end configuration of a solution path is not uniquely defined by hold g. Instead, the configurations that place the foot of the free limb at g form a 2-D subspace G of C_{ik}. No such configurations can be obtained by sampling C_{ik} at random. So, the planner specifically samples configurations in G by sampling positions (x_p, y_p) of the pelvis in the intersection of the three discs of radius $2L$ centered at holds i, k, and g, respectively. For each value of (x_p, y_p) a straightforward inverse-kinematics operation yields two values of the joint angles (θ_1, θ_2) of the free limb.

Algorithm 1 presents the overall method, where V and E denote the sets of vertices and edges of the roadmap, respectively, and N_1 and N_2 are input parameters used to bound the computation. Notice that hold g usually must be reached so that the robot can use holds i and g (or k and g) as supporting holds for a subsequent move. Thus, the equilibrium test at Step 3b only retains goal configurations that lie in $F_{ik} \cap F_{ig}$ or $F_{ik} \cap F_{kg}$. An appropriate metric at Step 5b is the sum of the magnitudes of the joint angle differences. Simple smoothing techniques [4] are used to improve the path produced by the algorithm.

Algorithm 1 One-Step-Climbing

1. $V \leftarrow \{\}$, $E \leftarrow \{\}$
2. If q_s satisfies the equilibrium test, then add q_s to V, else exit with failure.
3. (*Sample the goal region*) Loop N_1 times:
   (a) Sample uniformly at random a combination of knee bends of the contact chain and a pelvis position (x_p, y_p) within distance $2L$ from each of the three holds i, k, and g.
   (b) For each of the corresponding two configurations q where the foot of the free limb is at g, if q satisfies the equilibrium test, then add q to V.
4. If no vertex was added to V at Step 3, then exit with failure.
5. (*Sample the feasible space*) Loop N_2 times:
   (a) Sample uniformly at random a configuration $q \in F_{ik}$. If it satisfies the equilibrium test, then add q to V.
   (b) For every configuration q' previously in V that is closer to q than some predefined distance, if the linear path joining q and q' satisfies the equilibrium test, then add this path to E.
   (c) If the connected component containing q_s also contains a configuration sampled at Step 3 (goal configuration), then exit with a path.
6. Exit with failure.

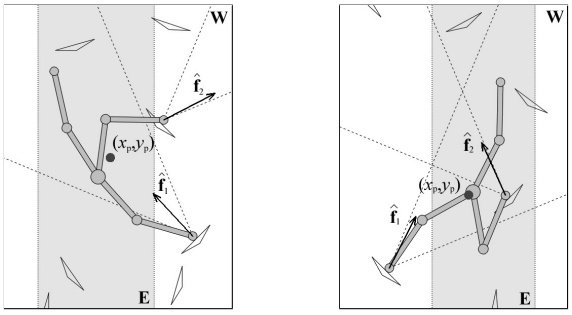

(a) Lie-Back (b) Back-Step

Fig. 4. Two configurations where the robot is in equilibrium.

3.3 Equilibrium test

The only external forces acting on the robot are gravity and the reaction forces at holds i and k. The gravitational force acts at the robot's center of mass (CM), the position of which varies as the robot moves. Hence, the equilibrium constraint restricts the range of positions of the CM.

Since the gravitational force has fixed magnitude and orientation, if the robot is in equilibrium at some configuration q in C_{ik} (hence, $q \in F_{ik}$) that places the CM at abscissa x_c, then the robot is in equilibrium at any configuration q' in C_{ik} that places the CM at the same abscissa. Let E denote the range of values of the abscissa of the CM where the robot is in equilibrium.

We extend the work of [36] to construct E. Assume that the robot has mass m, that the CM is located at (x_c, y_c), and that the gravitational force is $\boldsymbol{g} = (0, 0, -g)$. Let $\boldsymbol{r}_i = (x_i, y_i)$ and $\boldsymbol{r}_k = (x_k, y_k)$.

The reaction forces at the two holds i and k are constrained to vary within friction cones FC_i and FC_k. Define unit vectors $\hat{f}_{i1}, \hat{f}_{i2}$ along each edge of FC_i. The sum of any two contact forces $\boldsymbol{f}_{i1} = f_{i1}\hat{f}_{i1}$ and $\boldsymbol{f}_{i2} = f_{i2}\hat{f}_{i2}$ lies within FC_i if and only if $f_{i1}, f_{i2} \geq 0$. So, equilibrium can be expressed as the following linear equation:

$$\begin{bmatrix} \hat{f}_{i1} & \hat{f}_{i2} & \hat{f}_{k1} & \hat{f}_{k2} & 0 & 0 \\ \boldsymbol{r}_i \times \hat{f}_{i1} & \boldsymbol{r}_i \times \hat{f}_{i2} & \boldsymbol{r}_k \times \hat{f}_{k1} & \boldsymbol{r}_k \times \hat{f}_{k2} & 0 & 0 \\ & & & & -mg & 0 \end{bmatrix} \begin{bmatrix} f_{i1} \\ f_{i2} \\ f_{k1} \\ f_{k2} \\ x_c \\ y_c \end{bmatrix} = \begin{bmatrix} 0 \\ mg \\ 0 \end{bmatrix} \tag{1}$$

As mentioned above, Eq. 1 has zero dependence on y_c. E is the set of all x_c feasible under this relation, with the additional constraint that all $f_{ij}, f_{kj} \geq 0$.

Let $\mathbf{M}$ be the first matrix of Eq. 1. If $\mathbf{M}$ were full-rank, Eq. 1 would have a unique solution (if any). However, there is often some redundancy in choosing f_{ij}, f_{kj} and x_c. Let $\mathbf{M}^{-1}$ be the right pseudo-inverse of $\mathbf{M}$ and let $\mathbf{N}$ be a basis for the null space of $\mathbf{M}$. We re-write Eq. 1 as follows, where η is a vector of dimension dim(null($\mathbf{M}$)):

$$\begin{bmatrix} f_{i1} \\ f_{i2} \\ f_{k1} \\ f_{k2} \\ x_c \\ y_c \end{bmatrix} = \mathbf{M}^{-1} \begin{bmatrix} 0 \\ mg \\ 0 \end{bmatrix} + \mathbf{N}\eta \tag{2}$$

Further, let:

$$\mathbf{b} = \mathbf{M}^{-1} \begin{bmatrix} 0 \\ mg \\ 0 \end{bmatrix} \quad \text{and} \quad \boldsymbol{f} = \begin{bmatrix} f_{i1} \\ f_{i2} \\ f_{k1} \\ f_{k2} \end{bmatrix} \tag{3}$$

Finally, express Eq. 2 in block form as:

$$\boldsymbol{f} = \mathbf{N}_1\eta + \mathbf{b}_1 \tag{4}$$

$$\begin{bmatrix} x_c \\ y_c \end{bmatrix} = \mathbf{N}_2\eta + \mathbf{b}_2 \tag{5}$$

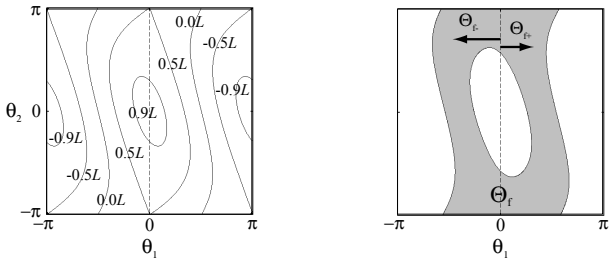

(a) (b)

Fig. 5. Space Θ.

To find all possible positions of the CM, we first find all η satisfying Eq. 4, then project this solution space through Eq. 5. The linear equality yields a polytope of dimension dim(null(**M**)) by an intersection of halfspaces. So, the region in η is convex, E is a single interval, and the region in (x_c, y_c) is a vertical column. Finding the region in η is the problem of *vertex enumeration* for a polyhedron in H-format, for which methods are available [14, 15].

To test a given configuration q sampled from C_{ik} for equilibrium, it suffices to compute E and the abscissa x_c of the CM for this configuration, and check if $x_c \in E$. Fig. 4 shows two configurations produced by our software. In each case, the column defined by E is the shaded region and the CM is the bold black dot. In the rock-climbing literature [18], the configuration on the left is a called a "lie-back" and the one on the right a "back-step" (compare to Fig. 1b). Note that in the lie-back configuration, the shaded column is entirely to the left of both holds.

To test that a linear path between two configurations q and q' keeps the robot in equilibrium, one may sample the path at some resolution and test sampled points for equilibrium. A better approach adapted from [49] is the following. Compute an upper-bound λ on the length of the path traced out by the CM when the robot configuration is linearly interpolated between q and q'. If at either q or q' the minimum distance between x_c and the bounds of E exceeds λ, then accept the path. Otherwise, set q_{mid} to $(q+q')/2$. If the robot is not in equilibrium at q_{mid}, then reject the path, else apply the same treatment recursively to the two sub-paths joining q and q_{mid}, and q_{mid} and q'.

3.4 Feasible space for a given configuration of the contact chain

Assume the contact chain is in a given configuration specified by the location (x_p, y_p) of the pelvis and its knee bends. Let $\Theta = \{(\theta_1, \theta_2) | \theta_1, \theta_2 \in [-\pi, \pi]\}$ denote the configuration space of the free limb and Θ_f the subset of Θ that corresponds to equilibrium configurations of the robot. Here we analyze the connectivity of Θ_f. It will result in a refined version of the algorithm of Section 3.2.

The abscissa x_c of the robot's CM must be in the interval $E = [x_{\min}, x_{\max}]$. Since the CM of the contact chain is fixed, this constraint can be transformed into a constraint on the CM of the free limb. Let $x_{c/chain}$ and $x_{c/free}$ denote the abscissas of the CM of the contact chain and the free limb, respectively. We have $x_{c/free} = 3x_c - 2x_{c/chain}$, so $x_{c/free}$ must lie in the interval $(x_{min/free}, x_{max/free})$, where:

$$x_{min/free} = 3x_{min} - 2x_{c/chain} \quad \text{and} \quad x_{max/free} = 3x_{max} - 2x_{c/chain} \tag{6}$$

The abscissa of the CM of the free limb can be expressed as:

$$x_{c/free} = x_p + \frac{L}{4}(3\cos\theta_1 + \cos(\theta_1 + \theta_2)) \tag{7}$$

When θ_1 and θ_2 span Θ, $\delta = x_{c/free} - x_p$ ranges between $-L$ and L. The values of θ_1 and θ_2 that are solutions of Eq. 7 for any $\delta \in [-L, L]$ define a curve in Θ. Since the mapping from (θ_1, θ_2) to Θ is single-valued, no two such curves intersect. Fig. 5a shows these curves for $\delta = -0.9L, -0.5L, 0, 0.5L$, and $0.9L$ for some configuration of the contact chain. The subset Θ_f is the region between the two curves defined by $\delta_{min} = x_{min/free} - x_p$ and $\delta_{max} = x_{max/free} - x_p$. It is shown in Fig. 5b (shaded area), where the configuration of the contact chain yields $\delta_{min} = -0.1L$ and $\delta_{max} = 0.7L$.

Θ_f is empty if and only if $[\delta_{min}, \delta_{max}] \cap [-L, L]$ is empty. So, for given knee bends of the contact chain, a pelvis location is feasible with respect to the robot's equilibrium constraint if:

$$\delta_{min} < L \quad \text{and} \quad \delta_{max} > -L \tag{8}$$

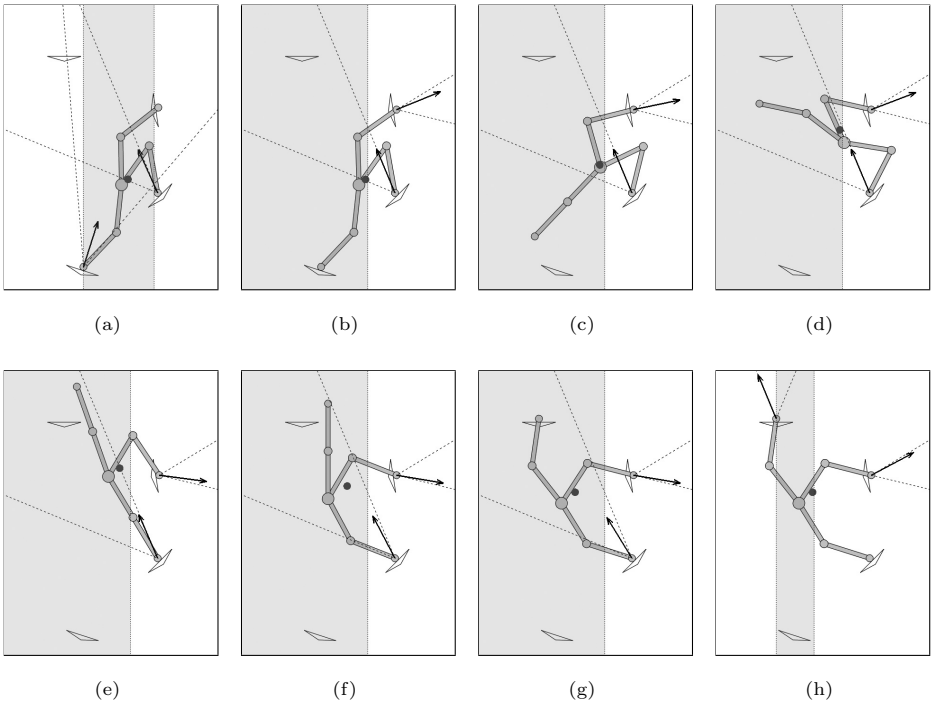

Fig. 6. Example of motion computed by Alg. 1 for the three-limbed robot.

When Eq. 8 is satisfied, we divide Θ_f into two subsets: Θ_{f-}, where $\theta_1 \leq 0$ (the first link of the free limb points downward), and Θ_{f+}, where $\theta_1 \geq 0$ (the first link points upward). For any given $\delta \in [\delta_{min}, \delta_{max}] \cap [-L, L]$, the values of θ_1 and θ_2 that are solutions of Eq. 7 form a single continuous curve segment in Θ_{f-} and another one in Θ_{f+}. Since no two curves for distinct values of δ intersect, Θ_{f-} and Θ_{f+} are each connected. In addition, since $(\theta_1, \theta_2) = (-\cos^{-1}(\delta/L), 0)$ and $(\theta_1, \theta_2) = (\cos^{-1}(\delta/L), 0)$ are solutions of Eq. 7, they belong to Θ_{f-} and Θ_{f+}, respectively. So, each of the two segments defined by $\Theta_{f-} \cap \{\theta_2 = 0\}$ and $\Theta_{f+} \cap \{\theta_2 = 0\}$ span all feasible values of δ. Similarly, if two configurations (θ_1, θ_2) and (θ'_1, θ'_2) correspond to the same $\delta = \delta'$ and both belong to Θ_{f-} (resp., Θ_{f+}), a line of constant δ joining them lies entirely in Θ_{f-} (resp., Θ_{f+}).

It follows from the last statement that Θ_f is connected if and only if there exists θ_2 such that $(0, \theta_2)$ or $(\pm\pi, \theta_2)$ belongs to both Θ_{f-} and Θ_{f+}. This is the case if and only if at least one of the following conditions holds:

$$\delta_{min} \notin [-L/2, L/2] \quad \text{or} \quad \delta_{max} \notin [-L/2, L/2] \tag{9}$$

3.5 Motion computation (refined version)

Hence, any feasible continuous path of the contact chain can be lifted into F_{ik} by letting the free limb move in either Θ_{f-} or Θ_{f+}. This remark yields a refined version of Alg. 1 that only samples the 2-D pelvis location space, instead of the 4-D feasible space F_{ik}.

More precisely, Step 5 samples N_2 pelvis locations (and combinations of knee bends of the contact chain). Each sample satisfying Eq. 8 is lifted to two configurations $q_1, q_2 \in F_{ik}$ by computing the corresponding free limb's configurations in Θ_{f-} and Θ_{f+} at $\theta_2 = 0$. Also, if Eq. 9 is satisfied (i.e., if Θ_f is connected) the pelvis position is also lifted to a third configuration q_3 where the joint angle θ_1 of the free limb is either 0 or $\pm\pi$. These configurations are added to the set V of vertices of the roadmap. Whenever a configuration q_3 is generated, it is immediately connected to both q_1 and q_2 in the roadmap. The purpose of adding q_3 is to allow changes in the sign of θ_1. At Step 5b, the algorithm only tries to connect pairs of configurations with different (x_p, y_p), since the other connections have already been created.

The sampling of the goal region at Step 3 is unchanged. However, for each sampled pelvis position, the algorithm also adds two or three configurations q_1, q_2, and q_3 to V as above, and connects q_1 to q_3 and q_2 to q_3. Each of the two goal configurations created at Step 3b is also immediately connected to each of the configurations q_1, q_2, and q_3, for which the free limb is in the same component Θ_{f-} or Θ_{f+}. Step 2 is modified in the same way.

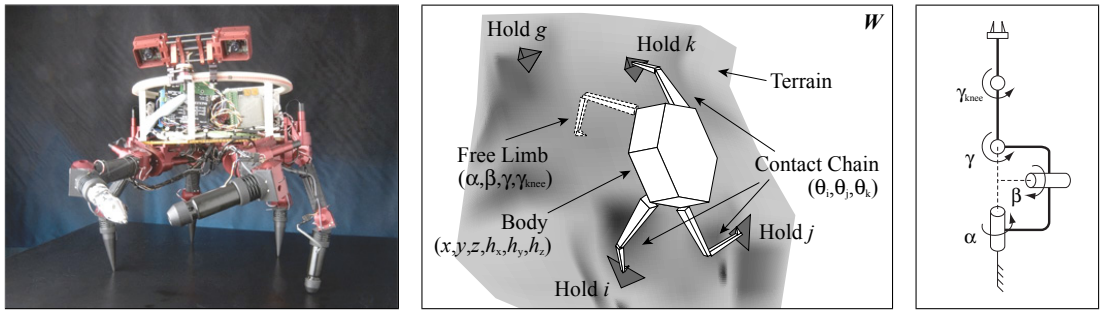

(a) LEMUR II (courtesy of the Planetary Robotics Laboratory, JPL)

(b) Robot model

(c) Limb model

Fig. 7. The 3-D four-limbed robot.

3.6 Simulation results

We have implemented the refined version of Alg. 1 for the three-limbed robot. Fig. 6 shows snapshots along a path computed by this software. The friction cone at each hold has a half-angle $\varphi = \pi/8$. The goal is for one limb endpoint to reach the upper-most hold. Frames 6b-6g show the motion along the path, during which the robot is standing on the two right-most holds. Frames 6a and 6h show the robot configuration immediately before the transition to the initial configuration and immediately after the transition to the initial configuration of the next move. Both the friction cones and the direction of the reaction forces at the supporting holds are shown in each frame. As required, the forces remain within the friction cones at all times. Likewise, the CM remains in the region E. A graphic animation of a sequence of climbing moves computed by the algorithm can be downloaded from `http://arl.stanford.edu/~tbretl/`.

We have run the software on many examples. The produced motion is often closely related to well-known human climbing techniques (e.g., Fig. 6 begins with a high-step and moves through lie-back configurations). On average, the size of the roadmap needed to find a path is small, because F_{ij} is usually "well-connected." Narrow passages can occur in F_{ij}, but most of them exist only in the entire 4-D space, not in the 2-D space of pelvis positions. The deterministic algorithm used in the refined version of the planner for generating free limb motions allows these passages to be traversed without search. Disconnections occasionally occur in F_{ij} when supporting holds are poorly positioned or oriented relative to each other, and/or their friction cones are narrow.

4 3-D Four-Limbed Robot

4.1 Description of robot

The robot is modeled after the LEMUR II robot shown in Fig. 7a [27, 28]. The original LEMUR II robot consists of six identical limbs attached to a hexagonal chassis. We intend to retain only four limbs for our initial hardware experiments, although the techniques presented below apply to any number of limbs. Thus, our model has only four limbs (Fig. 7b). We also assume that small hooks have been added to each limb endpoint, so that the robot can both push and pull on holds.

Each limb (Fig. 7c) has one spherical joint at the shoulder, which consists of three collocated revolute joints in ZYX-Euler sequence, and one revolute joint at the knee, which is parallel to the third axis of rotation at the shoulder (X). The joints are limited by internal mechanical stops, such that $\alpha \in [-\pi, \pi]$, $\beta \in [-\pi/2, \pi/2]$, $\gamma \in [-\pi/2, 0]$, and $\gamma_{\text{knee}} \in [-3\pi/4, 0]$. Each limb has length 30cm and mass 1kg. The chassis has radius 18.5cm and mass 3kg.

The robot moves in a 3-D space W. A fixed coordinate system O_{xyz} is embedded in W, with gravity pointing in the negative direction of the z-axis. Each hold i in W is defined by a point (x_i, y_i, z_i) and a direction ν_i. During a one-step motion, three limb endpoints of the robot are in contact with supporting holds, while one limb (the free limb) is moving. The linkage between the supporting holds is still called the contact chain. The motion takes place in a 13-D space C_{ik}, since the fixed positions of three feet reduce the number of DOF's of the contact chain to 9. As in the planar case, friction at each hold is modeled using Coulomb's law. But unlike in the planar case, the robot's self-collision and collision with the environment are not allowed.

4.2 Motion computation

The algorithm to plan one-step climbing moves for the 3-D robot is essentially Alg. 1 presented in Section 3.2, with the following modifications:

1. The joint limits are such that the inverse kinematics of each limb has at most one solution. Therefore, no decomposition of C_{ik} according to knee bends is needed.
2. Sampling configurations of the contact chain is much harder than in the planar case, so we now use a technique similar to those presented in [10, 20, 33].
3. The equilibrium test of Section 3.3 is modified slightly, as described in Section 4.3.
4. We used PQP [17] to check for both self-collision of the robot and collision with the environment.

The refined version of Section 3.5 does not scale directly to handle free limbs with more than 2 DOF's or additional constraints such as collision avoidance and joint limits.

4.3 Equilibrium test

As in the planar case, the only external forces acting on the robot are gravity and the reaction forces at three holds i, j, and k. Analogous to the planar case, if the robot is in equilibrium at some configuration $q \in C_{ijk}$ that places the CM at (x_c, y_c, z_c), then the robot is in equilibrium at any configuration $q' \in C_{ijk}$ such that $z'_c = z_c$. Let E denote the range of values of the coordinates (x_c, y_c) of the CM where the robot is in equilibrium.

Assume that the robot has mass m, that the CM is located at (x_c, y_c, z_c), and that the gravitational force is $\boldsymbol{g} = (0, 0, -g)$. Let $\boldsymbol{r}_h = (x_h, y_h, z_h)$ for holds $h = i, j, k$. The reaction force at each hold h is constrained to vary with a friction cone FC_h. However, we define a conservative approximation to FC_h as an n-gonal pyramid. This approximation can be made arbitrarily precise by increasing n (in our implementation, $n = 4$). Define unit vectors $\hat{f}_{h1}, \ldots, \hat{f}_{hn}$ along each edge of the pyramid. The sum of n contact forces $\boldsymbol{f}_{h1} = f_{h1}\hat{f}_{h1}, \ldots, \boldsymbol{f}_{h1} = f_{hn}\hat{f}_{hn}$ lies within the pyramid approximating FC_h if and only if all $f_{h1}, \ldots, f_{hn} \geq 0$. Therefore, we replace the friction cone constraint on each reaction force by this linear constraint on n contact forces, defined as above for each hold h.

Let $\boldsymbol{f}_h = (f_{h1}, \ldots, f_{hn})$ and define the following matrix for each hold h:

$$\boldsymbol{A}_h = \begin{bmatrix} \hat{f}_{h1} & \cdots & \hat{f}_{hn} \\ \boldsymbol{r}_h \times \hat{f}_{h1} & & \boldsymbol{r}_h \times \hat{f}_{hn} \end{bmatrix} \tag{10}$$

Then the equilibrium equations can be expressed as follows:

$$\begin{bmatrix} & & & 0 & 0 & 0 \\ & & & 0 & 0 & 0 \\ & & & 0 & 0 & 0 \\ \boldsymbol{A}_i & \boldsymbol{A}_j & \boldsymbol{A}_k & 0 & -mg & 0 \\ & & & mg & 0 & 0 \\ & & & 0 & 0 & 0 \end{bmatrix} \begin{bmatrix} \boldsymbol{f}_i \\ \boldsymbol{f}_j \\ \boldsymbol{f}_k \\ x_c \\ y_c \\ z_c \end{bmatrix} = \begin{bmatrix} 0 \\ 0 \\ mg \\ 0 \\ 0 \\ 0 \end{bmatrix} \tag{11}$$

This equation has zero dependence on z_c. Finding the region E from Eq. 11 follows identically the process described in Section 3.3. E is a convex polygonal region and the region in (x_c, y_c, z_c) is the vertical column whose cross-section is E. To test a given configuration q sampled from C_{ik} for equilibrium, we compute E and the projection (x_c, y_c) of the CM for this configuration, and we check if $(x_c, y_c) \in E$. Testing linear paths between two configurations is done as in Section 3.3.

This analysis can easily be extended to cases where the robot is supported by arbitrary many holds, simply by modifying Eq. 1 and 11.

4.4 Simulation results

Fig. 8a-8e shows snapshots of a one-step motion computed by our algorithm. In this example, the robot moves out of a "cross-through" limb position to reach for the left-most hold, on 3-D terrain with a slight overhang. During the motion, the robot rotates its pelvis, but maintains a "backstep" configuration with its two bottom limbs in order to keeps its CM within E (not shown). Fig. 8f-8j shows snapshots of a human climber executing a similar motion. The climber also maintains a "backstep" configuration, and turns his torso to reach for the left-most hold just as the robot does.

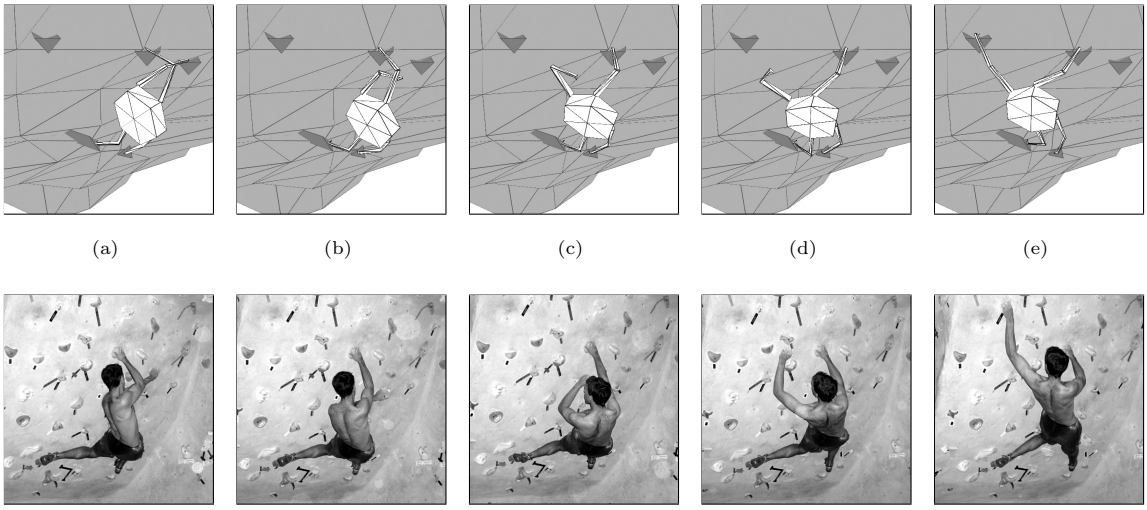

Fig. 8. Example of motion computed by Alg. 1 for the 3-D four-limbed robot.

5 Future Work

This paper presented a PRM planning algorithm—One-Step-Climbing—to compute the motion of a multi-limbed robot climbing vertical terrain. To prevent the robot from falling as it moved a limb to reach a new hold, the algorithm exploits friction at supporting holds and adjusted the robot's internal degrees of freedom. This algorithm was demonstrated in simulation for a planar three-limbed robot and for a 3-D four-limbed robot modeled after the LEMUR II robot created by JPL. Many trajectories computed by this algorithm has striking similarities with classical moves developed by human climbers. The basic algorithm is fast enough to be used on-line. Nevertheless, in the case of the three-limbed robot, an analysis of the geometry of the robot's feasible space made it possible to capture narrow passages more efficiently by only sampling a subspace of the feasible space. We hope to extend this improvement to the four-limbed robot.

We are currently working on applying the One-Step-Climbing algorithm to the four-limbed version of LEMUR II, in a real hardware experiment. To accomplish this, additional constraints need to be considered that are ignored in the current software. For example, the algorithm will have to compute torques and reject configurations where torque limits are exceeded.

Enabling multi-limbed robots to climb natural vertical terrain raises many other challenging problems not addressed in this paper. Sensing, grasping, and control are prominent among them. Visual and tactile sensing will be needed to localize and test potential holds. In natural terrain, holds are not just points, but 3-D features that can be "grasped" in many different ways [8]. Closed-loop motion control, using tactile feedback (slippage detection), should be developed to adjust computed paths during execution. Multi-step planning [9] based on incomplete information about the terrain ahead will also be needed to choose which hold to reach next, when multiple holds are within reach.

Acknowledgements. T. Bretl is partially supported by a Herbert Kunzel Fellowship. The authors would like to thank D. Halperin, T. Miller, and M. Moll for their helpful comments. In particular, they would like to thank B. Kennedy and E. Baumgartner of the Planetary Robotics Laboratory at JPL for their contributions.

References

[1] H. Amano, K. Osuka, and T.-J. Tarn. Development of vertically moving robot with gripping handrails for fire fighting. In *IEEE/RSJ Int. Conf. on Intelligent Robots and Systems*, Maui, HI, 2001.

[2] K. Autumn, M. Sitti, Y. Liang, A. Peattie, W. Hansen, S. Sponberg, T. Kenny, R. Fearing, J. Israelachvili, and R. Full. Evidence for van der waals adhesion in gecko setae. *PNAS*, 99(19):11252–12256, Jan 1999. http://www.pnas.org/content/vol99/issue19/cover.shtml.

[3] J. E. Bares and D. S. Wettergreen. Dante ii: Technical description, results and lessons learned. *Int. J. of Robotics Research*, 18(7):621–649, 1999.

[4] J. Barraquand and J. Latombe. Robot motion planning: A distributed representation approach. *Int. J. of Robotics Research*, 10(6):628–649, 1991.

[5] D. Bevly, S. Farritor, and S. Dubowsky. Action module planning and its application to an experimental climbing robot. In *IEEE Int. Conf. on Robotics and Automation*, volume 4, pages 4009–4014, 2000.

[6] A. Bicchi and V. Kumar. Robotic grasping and contact: A review. In *IEEE Int. Conf. on Robotics and Automation*, pages 348–353, San Francisco, CA, 2000.

[7] J.-D. Boissonnat, O. Devillers, and S. Lazard. Motion planning of legged robots. *SIAM J. on Computing*, 30(1):218–246, 2001.

[8] T. Bretl, T. Miller, S. Rock, and J.-C. Latombe. Climbing robots in natural terrain. In *i-SAIRAS*, Nara, Japan, May 2003.

[9] T. Bretl, S. Rock, and J.-C. Latombe. Motion planning for a three-limbed climbing robot in vertical natural terrain. In *IEEE Int. Conf. on Robotics and Automation*, Taipei, Taiwan, 2003.

[10] J. Cortes, T. Simeon, and J. Laumond. A random loop generator for planning the motions of closed kinematic chains using prm methods. In *IEEE Int. Conf. on Robotics and Automation*, Washington, D.C., 2002.

[11] A. V. der Stappen, C. Wentink, and M. Overmars. Computing form-closure configurations. In *IEEE Int. Conf. on Robotics and Automation*, pages 1837–1842, 1999.

[12] C. Eldershaw and M. Yim. Motion planning of legged vehicles in an unstructured environment. In *IEEE Int. Conf. on Robotics and Automation*, Seoul, South Korea, 2001.

[13] T. Estier, Y. Crausaz, B. Merminod, M. Lauria, R. Pguet, and R. Siegwart. An innovative space rover with extended climbing abilities. In *Space and Robotics*, Albuquerque, NM, 2000.

[14] K. Fukuda. cdd+ reference manual. Technical report, Institute for Operations Research, Swiss Federal Institute of Technology, Zurich, Switzerland, 1995. http://www.ifor.math.ethz.ch/~fukuda/fukuda.html.

[15] K. Fukuda and A. Prodon. Double description method revisited. *LNCS*, 1120:91–111, 1996.

[16] K. Gopalakrishnan and K. Goldberg. Gripping parts at concave vertices. In *IEEE Int. Conf. on Robotics and Automation*, 2001.

[17] S. Gottschalk, M. Lin, and D. Manocha. Obb-tree: A hierarchical structure for rapid interference detection. In *ACM SIGGRAPH*, pages 171–180, 1996.

[18] D. Graydon and K. Hanson. *Mountaineering: The Freedom of the Hills*. Mountaineers Books, 6th rev edition, Oct 1997.

[19] J. C. Grieco, M. Prieto, M. Armada, and P. G. d. Santos. A six-legged climbing robot for high payloads. In *IEEE Int. Conf. on Control Applications*, Trieste, Italy, 1998.

[20] L. Han and N. Amato. A kinematics-based probabilistic roadmap method for closed chain systems. In *Int. Workshop on Algorithmic Foundations of Robotics*, 2000.

[21] S. Hirose and O. Kunieda. Generalized standard foot trajectory for a quadruped walking vehicle. *Int. J. of Robotics Research*, 10(1):3–12, 1991.

[22] S. Hirose, A. Nagabuko, and R. Toyama. Machine that can walk and climb on floors, walls, and ceilings. In *5th Int. Conf. on Advanced Robotics*, pages 753–758, Pisa, Italy, 1991.

[23] S. Hirose, K. Yoneda, and H. Tsukagoshi. Titan vii: Quadruped walking and manipulating robot on a steep slope. In *IEEE Int. Conf. on Robotics and Automation*, Albuquerque, NM, 1997.

[24] K. Iagnemma, A. Rzepniewski, S. Dubowsky, P. Pirjanian, T. Huntsberger, and P. Schenker. Mobile robot kinematic reconfigurability for rough-terrain. In *Sensor Fusion and Decentralized Control in Robotic Systems III*, volume 4196 of *SPIE*, Boston, MA, 2000.

[25] iRobot. Gecko wall climbing robot: Component technologies for climbing. http://www.irobot.com/rd/p05_Gecko.asp.

[26] L. E. Kavraki, P. Svetska, J.-C. Latombe, and M. Overmars. Probabilistic roadmaps for path planning in high-dimensional configuration spaces. *IEEE Tr. on Robotics and Automation*, 12(4):566–580, 1996.

[27] B. Kennedy, H. Aghazarian, Y. Cheng, M. Garrett, G. Hickey, T. Huntsberger, L. Magnon, C. Mahoney, A. Meyer, and J. Knight. Lemur: Legged excusion mechanical utility rover. *Autonomous Robots*, 11:201–205, 2001.

[28] B. Kennedy, A. Okon, H. Aghazarian, M. Robinson, M. Garrett, and L. Magnon. Second generation six-limbed robot. Technical Report NPO-35140, NASA, 2003. http://prl.jpl.nasa.gov/.

[29] E. Krotkov and R. Simmons. Perception, planning, and control for autonomous walking with the ambler planetary rover. *Int. J. of Robotics Research*, 15:155–180, 1996.

[30] J. Kuffner, J., K. Nishiwaki, S. Kagami, M. Inaba, and H. Inoue. Footstep planning among obstacles for biped robots. In *IEEE/RSJ Int. Conf. on Intelligent Robots and Systems*, Maui, HI, 2001.

[31] J. Kuffner, J., K. Nishiwaki, S. Kagami, M. Inaba, and H. Inoue. Motion planning for humanoid robots under obstacle and dynamic balance constraints. In *IEEE Int. Conf. on Robotics and Automation*, 2001.

[32] V. Kumar and K. Waldron. Gait analysis for walking machines for omnidirectional locomotion on uneven terrain. In *7th Symp. on Theory and Practice of Robots and Manipulators*, pages 47–67, 1988.

[33] S. LaValle, J. Yakey, and L. Kavraki. A probabilistic roadmap approach for systems with closed kinematic chains. In *IEEE Int. Conf. on Robotics and Automation*, Detroit, MI, 1999.

[34] A. Madhani and S. Dubowsky. Motion planning of mobile multi-limb robotic systems subject to force and friction constraints. In *IEEE Int. Conf. on Robotics and Automation*, volume 1, pages 233–239, Nice, France, 1992.

[35] K. Markenscoff, L. Ni, and C. Papadimitriou. The geometry of grasping. *Int. J. of Robotics Research*, 9(1):61–73, 1990.

[36] R. Mason, E. Rimon, and J. Burdick. Stable poses of 3-dimensional objects. In *IEEE Int. Conf. on Robotics and Automation*, Albuquerque, NM, 1997.

[37] R. McGhee and S. Sun. On the problem of selecting a gait for a legged vehicle. In *Tr. of the VI IFAC Symp.*, pages 53–62, 1974.

[38] B. Mishra, J. Schwartz, and M. Sharir. On the existence and synthesis of multifinger positive grips. *Algorithmica*, 2(4):541–558, 1987.

[39] W. Neubauer. A spider-like robot that climbs vertically in ducts or pipes. In *IEEE/RSJ/GI Int. Conf. on Intelligent Robots and Systems*, pages 1178–1185, Munich, Germany, 1994.

[40] V. Nguyen. Constructing force-closure grasps. *Int. J. of Robotics Research*, 7(3):3–16, 1998.

[41] M. Nilsson. Snake robot - free climbing. *IEEE Control Systems Magazine*, 18(1):21–26, Feb 1998.

[42] D. Pai, R. Barman, and S. Ralph. Platonic beasts: Spherically symmetric multilimbed robots. *Autonomous Robots*, 2(4):191–201, 1995.

[43] P. Pirjanian, C. Leger, E. Mumm, B. Kennedy, M. Garrett, H. Aghazarian, S. Farritor, and P. Schenker. Distributed control for a modular, reconfigurable cliff robot. In *IEEE Int. Conf. on Robotics and Automation*, Washington, D.C., 2002.

[44] J. Ponce, J. Burdick, and E. Rimon. Computing the immobilizing three-finger grasps of planar objects. In *Workshop on Computational Kinematics*, 1995.

[45] E. Rimon, S. Shoval, and A. Shapiro. Design of a quadruped robot for motion with quasistatic force constraints. *Autonomous Robots*, 10:279–296, 2001.

[46] R. Rimon and J. Burdick. On force and form closure for multiple finger grasps. In *IEEE Int. Conf. on Robotics and Automation*, 1996.

[47] Z. M. Ripin, T. B. Soon, A. B. Abdullah, and Z. Samad. Development of a low-cost modular pole climbing robot. In *TENCON*, volume 1, pages 196–200, Kuala Lumpur, Malaysia, 2000.

[48] T. Roßmann and F. Pfeiffer. Control of an eight legged pipe crawling robot. In *Int. Symp. on Experimental Robotics*, pages 353–346, 1997.

[49] F. Schwarzer, M. Saha, and J. Latombe. Exact collision checking of robot paths. In *Workshop on Algorithmic Foundations of Robotics*, Nice, France, Dec 2002.

[50] R. Simmons, E. Krotkov, L. Chrisman, F. Cozman, R. Goodwin, M. Hebert, L. Katragadda, S. Koenig, G. Krishnaswamy, Y. Shinoda, W. R. L. Whittager, and P. Klarer. Experience with rover navigation for lunar-like terrains. In *Intelligent Robots and Systems*, pages 441–446. IEEE, 1995.

[51] D. Wettergreen, H. Thomas, and C. Thorpe. Planning strategies for the ambler walking robot. In *IEEE Int. Conf. on Systems Engineering*, 1990.

[52] Y. Xu, H. Brown, M. Friendman, and T. Kanade. Control system of the self-mobile space manipulator. *IEEE Tr. On Control Systems Technology*, 2(3):207–219, 1994.

[53] M. Yim. A reconfigurable modular robot with many modes of locomotion. In *JSME Int. Conf. on Advanced Mechatronics*, Tokyo, Japan, 1993.

[54] M. Yim, S. homans, and K. Roufas. Climbing with snake-robots. In *IFAC Workshop on Mobile Robot Technology*, Jejudo, Korea, 2001.

[55] K. Yoneda, F. Ito, Y. Ota, and S. Hirose. Steep slope locomotion and manipulation mechanism with minimum degrees of freedom. In *IEEE/RSJ Int. Conf. on Intelligent Robots and Systems*, pages 1897–1901, 1999.

[56] K. Yoneda, Y. Ota, and S. Hirose. Development of a hi-grip stair climbing crawler with hysteresis compliant blocks. In *4th Int. Conf. on Climbing and Walking Robots*, pages 569–576, 2001.